BMC Microbiology

BioMed Central

Research article

Open Access

Genomic homogeneity between *Mycobacterium avium* subsp. *avium* and *Mycobacterium avium* subsp. *paratuberculosis* belies their divergent growth rates

John P Bannantine*[1], Qing Zhang[2], Ling-Ling Li[2] and Vivek Kapur[2]

Address: [1]National Animal Disease Center, USDA-ARS, 2300 N. Dayton Ave., Ames, IA 50010, USA and [2]Biomedical Genomics Center and Departments of Microbiology and Veterinary Pathobiology, University of Minnesota, Minneapolis, MN, USA

Email: John P Bannantine* - jbannant@nadc.ars.usda.gov; Qing Zhang - qing@mail.ahc.umn.edu; Ling-Ling Li - lixxx068@gold.tc.umn.edu; Vivek Kapur - vkapur@tc.umn.edu

* Corresponding author

Published: 9 May 2003

BMC Microbiology 2003, **3**:10

Received: 5 December 2002

Accepted: 9 May 2003

This article is available from: http://www.biomedcentral.com/1471-2180/3/10

Abstract

Background: *Mycobacterium avium* subspecies *avium* (*M. avium*) is frequently encountered in the environment, but also causes infections in animals and immunocompromised patients. In contrast, *Mycobacterium avium* subspecies *paratuberculosis* (*M. paratuberculosis*) is a slow-growing organism that is the causative agent of Johne's disease in cattle and chronic granulomatous infections in a variety of other ruminant hosts. Yet we show that despite their divergent phenotypes and the diseases they present, the genomes of *M. avium* and *M. paratuberculosis* share greater than 97% nucleotide identity over large (25 kb) genomic regions analyzed in this study.

Results: To characterize genome similarity between these two subspecies as well as attempt to understand their different growth rates, we designed oligonucleotide primers from *M. avium* sequence to amplify 15 minimally overlapping fragments of *M. paratuberculosis* genomic DNA encompassing the chromosomal origin of replication. These strategies resulted in the successful amplification and sequencing of a contiguous 11-kb fragment containing the putative *Mycobacterium paratuberculosis* origin of replication (*oriC*). This fragment contained 11 predicted open reading frames that showed a conserved gene order in the *oriC* locus when compared with several other Gram-positive bacteria. In addition, a GC skew analysis identified the origin of chromosomal replication which lies between the genes *dnaA* and *dnaN*. The presence of multiple DnaA boxes and the ATP-binding site in *dnaA* were also found in *M. paratuberculosis*. The strong nucleotide identity of *M. avium* and *M. paratuberculosis* in the region surrounding the origin of chromosomal replication led us to compare other areas of these genomes. A DNA homology matrix of 2 million nucleotides from each genome revealed strong synteny with only a few sequences present in one genome but absent in the other. Finally, the 16s rRNA gene from these two subspecies is 100% identical.

Conclusions: We present for the first time, a description of the *oriC* region in *M. paratuberculosis*. In addition, genomic comparisons between these two mycobacterial subspecies suggest that differences in the *oriC* region may not be significant enough to account for the diverse bacterial replication rates. Finally, the few genetic differences present outside the origin of chromosomal replication in each genome may be responsible for the diverse growth rates or phenotypes observed between the *avium* and *paratuberculosis* subspecies.

Background

Mycobacteria are Gram-positive, acid-fast, pleomorphic, non-motile rods belonging to the order Actinomycetales. *Mycobacterium avium* complex organisms consist of the human and animal pathogens *M. avium* subsp. *avium*, *M. avium* subsp. *paratuberculosis*, and *M. avium* subsp. *silvaticum* [1]. DNA-DNA hybridization studies have long ago established a genetic similarity between *M. avium* subspecies *avium* (*M. avium*) and *M. avium* subspecies *paratuberculosis* (*M. paratuberculosis*) [2–4]. Now that whole genome sequencing technologies are available, investigators can begin to examine genetic relatedness in greater detail through direct nucleotide-nucleotide comparisons. These comparisons are particularly important in instances where two genetically similar bacteria have little or no specific diagnostic tests to distinguish each.

The literature reports genetic similarity between *M. paratuberculosis* and *M. avium* at between 72% and 95% [2,4] depending on the region analyzed. However, despite the reported similarities, these mycobacteria are quite different phenotypically. *M. paratuberculosis* is an intracellular pathogen that infects ruminant animals, most notably cattle and sheep. The site of infection is the gastrointestinal tract, where it causes a chronic inflammatory ailment termed Johne's disease [5]. In contrast, *M. avium* is common in the environment, causes tuberculosis in birds, and disseminated infections in HIV patients [6]. Growth of *M. paratuberculosis* is characterized by its slow rate (doubling time of 22–26 hours, compared to 10–12 hours for *M. avium*) and requirement of mycobactin in culture media [5]. With the absence of a well-defined genetic system for *M. paratuberculosis*, a comparative genomic approach holds great potential in addressing the genetic basis for many of these phenotypic differences.

The genus *Mycobacterium* contains species that range from fast-growingsaprophytes such as *M. smegmatis* and *M. fortuitum* to slow-growing pathogens such as*M. leprae*, *M. tuberculosis* and *M. paratuberculosis*. Although the chromosomal origin of replication has been studied in some mycobacteria [7,8], the genetic organization of the origin of replication in *M. paratuberculosis* has been previously unknown. Knowledge of the gene organization and sequence of this region is particularly important because chromosomal replication may be regulated by a common mechanism that could directly affect rate of growth.

Several features of the *oriC* region are highly conserved among bacteria. The sequence immediately flanking the *dnaA* gene is considered the origin of chromosomal replication, or *oriC* region [9,10]. This region contains several genes that encode proteins required for basic cellular functions, including the protein subunit of RNase P (RnpA), ribosomal protein L34 (RpmH), the replication initiator protein (DnaA), the beta subunit of DNA polymerase III (DnaN), the recombination repair protein RecF, and the DNA gyrase proteins GyrA and GyrB. The relative gene order in this region is also highly conserved in many bacteria, especially the Gram-positives [11]. Although intergenic sequences in this region are conserved only among closely related organisms, the DnaA box is found in the non-coding regions flanking *dnaA* in most bacteria studied [12]. DnaA boxes are conserved nucleotide sequences (TTGTCCACA) where the DnaA protein binds to DNA, triggering events that ultimately lead to replication initiation and DNA synthesis [9].

In an effort to understand the genetic basis for growth rate and other phenotypic differences between *M. paratuberculosis* and *M. avium*, we have analyzed the genetic similarity of these genomes using two strategies. First, the putative *oriC* region of *M. paratuberculosis* was amplified, sequenced and compared with *M. avium* and other bacteria. Second, we examined nucleotide identity outside the *oriC* region using DNA homology matrix analysis as well as using several hundred *M. paratuberculosis* sequences from a random shotgun library compared with *M. avium* sequences present in the unfinished microbial genomes database. Our results show that these subspecies not only have a conserved gene order surrounding the origin of chromosomal replication, but also have a high synteny and nucleotide identity throughout both genomes. In addition, this preliminary comparative survey of the genomes of *M. avium* and *M. paratuberculosis* show even greater similarity (97%) than the literature suggests (72% to 95%) [2].

Results

Identification of predicted ORFs encoding replication-related proteins

An ~11-kb contiguous genomic fragment from M. paratuberculosis was amplified and sequenced using 15 primer pairs designed from M. avium genomic sequence in the putative oriC region (Fig. 1). This strategy enabled the successful amplification of all 15 minimally overlapping fragments of ~800 bp in length for this region of the M. paratuberculosis chromosome. A putative replication origin was identified by GC skew analysis [14]. A strong inflection point in the GC plot marks this origin (Fig. 1). Eleven ORFs were identified using the gene prediction software Artemis [15] (release 3; The Sanger Centre http://www.sanger.ac.uk/Software/Artemis/). Similarity searches were conducted locally using the BLASTP algorithm through the Artemis interface. Seven of these ORFs have high identity to proteins essential for basic cellular processes, including replication, in other mycobacterial species (Table 1). The function of GidB is unknown, but it may have a role in cell division [11]. RNase P, which consists of the protein subunit RnpA and a catalytic RNA

Table 1: Sequence analysis of predicted ORFs in the *M. paratuberculosis oriC* region.

Protein	Length (amino acids)	Top BLASTP match	Expect Value
1	311	*gidB* (*M. tuberculosis*, 62% identity, 70% similarity)	5e-64
2	195	hypothetical protein Rv3920c (*M. tuberculosis*, 70% identity, 72% similarity)	1e-49
3	370	hypothetical protein Rv3921c (*M. tuberculosis*, 87% identity, 92% similarity)	1e-142
4	115	hypothetical protein Rv3922c (*M. tuberculosis*, 67% identity, 76% similarity)	2e-35
5	126	*rnpA* (*M. tuberculosis*, 49% identity, 58% similarity)	5e-21
6	146	*rpmH* (*M. tuberculosis*, 89% identity, 93% similarity)	4e-17
7	524	*dnaA* (*M. avium*, 89% identity, 89% similarity)	0.0
8	409	*dnaN* (*M. tuberculosis*, 78% identity, 83% similarity)	1e-173
9	385	*recF* (*M. tuberculosis*, 66% identity, 75% similarity)	1e-144
10	280	hypothetical protein Rv0004 (*M. tuberculosis*, 65% identity, 71% similarity)	1e-63
11	685	*gyrB* (*M. leprae*, 84% identity, 88% similarity)	0.0

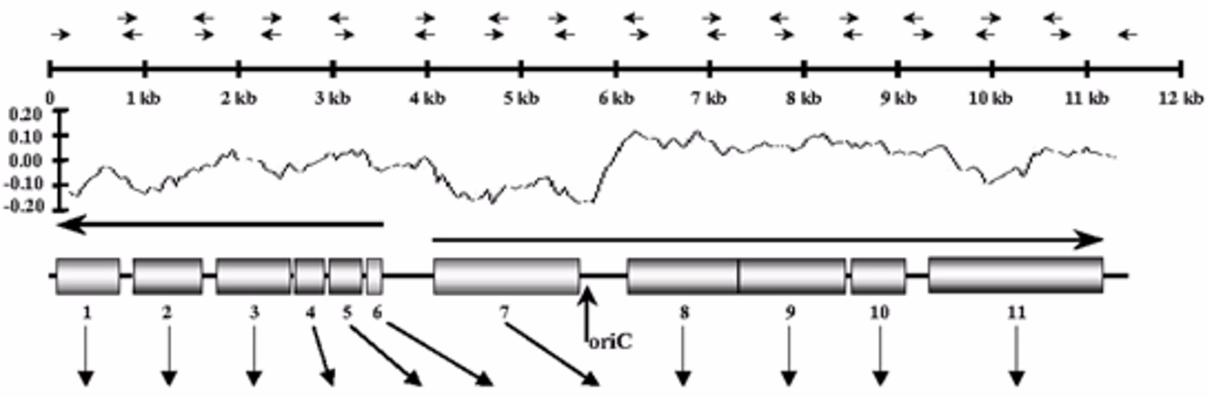

	gidB	unknown	unknown	unknown	rnpA	rpmH	dnaA	dnaN	recF	unknown	gyrB
π	0.011	0.007	0.007	0.010	0.027	0.000	0.007	0.010	0.019	0.017	0.008
ds	0.015	0.030	0.024	0.025	0.047	0.000	0.026	0.037	0.045	0.062	0.031
dn	0.010	0.000	0.001	0.005	0.019	0.000	0.001	0.000	0.009	0.000	0.001

Figure 1
Amplification strategy and organization of the *M. paratuberculosis* chromosomal origin of replication. The locations of primer pairs used for amplification and sequencing are marked with facing arrows above the kilobase (kb) scale. The GC skew is shown beneath the kb scale and has a window size of 500. OriC, right at the point of the GC inflection, designates the origin of replication. An open reading frame map of the ~11 kb fragment is represented by shaded boxes and the two divergent arrows immediately above identify the direction of transcription. The degree of substitution in comparison to the corresponding *M. avium* gene is indicated below the gene name. π (tau) is the overall substitution rate, ds is the synonymous substitution rate, and dn is the non-synonymous substitution rate. GidB, glucose inhibited division protein B. RnpA, RNAse protein component A. RpmH, ribosomal protein L34. DnaA, replication initiator. DnaN, DNA polymerase subunit III. GyrB, DNA gyrase subunit B.

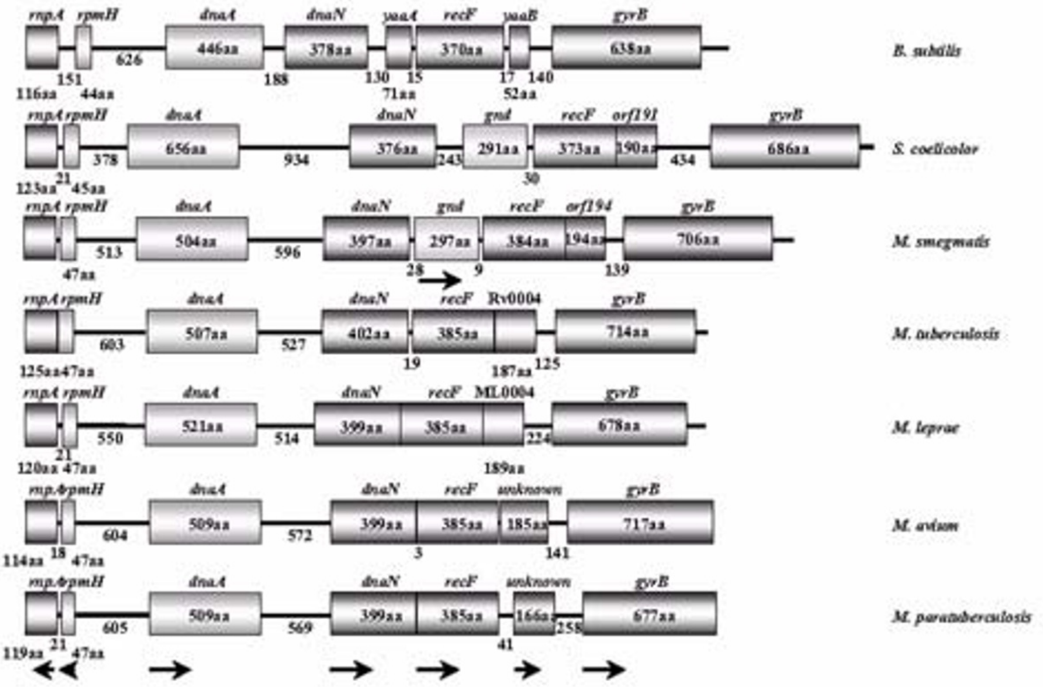
rnpA rpmH dnaA dnaN yaaA recF yaaB gyrB
626 446aa 378aa 370aa 638aa
B. subtilis
151 188 130 15 17 140
116aa 44aa 71aa 52aa
rnpA rpmH dnaA dnaN gnd recF orf191 gyrB
378 656aa 934 376aa 243 291aa 373aa 190aa 434 686aa
S. coelicolor
123aa 21 45aa 30
rnpA rpmH dnaA dnaN gnd recF orf194 gyrB
513 504aa 596 397aa 297aa 384aa 194aa 706aa
M. smegmatis
47aa 28 9 139
rnpA rpmH dnaA dnaN recF Rv0004 gyrB
603 507aa 527 402aa 385aa 714aa
M. tuberculosis
125aa47aa 19 187aa 125
rnpA rpmH dnaA dnaN recF ML0004 gyrB
550 521aa 514 399aa 385aa 224 678aa
M. leprae
21
120aa 47aa 189aa
rnpArpmH dnaA dnaN recF unknown gyrB
604 509aa 572 399aa 385aa 185aa 717aa
M. avium
114aa 18 47aa 3 141
rnpArpmH dnaA dnaN recF unknown gyrB
605 509aa 569 399aa 385aa 166aa 258 677aa
M. paratuberculosis
119aa 21 47aa 41

Figure 2

Comparative gene order in the *oriC* region of mycobacteria and other Gram-positive bacteria. The relative gene order in this region of *M. paratuberculosis* conforms to the highly conserved order found in other gram-positive bacteria. Numbers indicate the length of the ORF or intergenic region. Arrows show the direction of transcription.

subunit, is essential for generating mature tRNAs by cleaving the 5'-terminal leader sequences of precursor tRNAs [16]. rpmH encodes ribosomal protein L34, and DnaA is the initiator protein for chromosome replication. The B-subunit of DNA polymerase is encoded by dnaN. The recF gene product is involved in recombination, DNA repair, and induction of the SOS response, and may also have a role in replication [17]. Bacterial DNA gyrase, a tetramer consisting of A and B subunits, catalyzes the ATP-dependent unwinding of covalently closed circular DNA [18]. The remaining predicted ORFs in this region have high similarity to hypothetical proteins from M. tuberculosis (Table 1).

Sequence homology and conserved gene order in the oriC *region of mycobacteria and other gram-positive bacteria*

Alignment of the region surrounding oriC for several mycobacteria and other gram-positive bacteria provides some interesting comparisons (Fig. 2). The M. paratuberculosis oriC region conforms to the conserved gene order that is present in other mycobacteria as well as the closely related Streptomyces coelicolor. Even the more distantly related Bacillus subtilis shows some degree of synteny in this region. The fast growing M. smegmatis species contains a gnd sequence between dnaN and recF, which is absent in the slow-growing mycobacteria (Fig. 2). However, there appear to be no notable differences between M. avium and M. paratuberculosis at this level. The M. smegma-

Table 2: Comparison of amino acid identity in the *oriC* region with the corresponding *M. paratuberculosis* sequence.

	M. avium	*M. leprae*	*M. tuberculosis*	*M. smegmatis*	*S. coelicolor*	*C. glutamicum*
gidB	97% (98%)	66% (75%)	73% (83%)	Not Found	50% (64%)	51% (64%)
dnaN	100% (100%)	85% (88%)	86% (91%)	80% (89%)	51% (67%)	48% (69%)
rpmH	97% (100%)	91 % (95%)	91% (93%)	91% (95%)	81% (87%)	89% (93%)
Unknown (AAF33691)	100% (100%)	73% (82%)	85% (88%)	Not Found	64% (71%)	Not Found
dnaA	99% (99%)	87% (89%)	88% (90%)	78% (84%)	68% (78%)	53% (67%)
recF	97% (98%)	78% (87%)	76% (85%)	73% (84%)	55% (70%)	53% (71%)
gyrB	99% (100%)	90% (95%)	90% (94%)	88% (92%)	65% (79%)	72% (82%)
rnpA	94% (97%)	62% (76%)	60% (74%)	Not Found	41% (57%)	38% (56%)
unknown (AAF33696)	100% (100%)	78% (85%)	79% (88%)	70% (82%)	39% (51%)	33% (47%)
unknown (AAF33697)	98% (98%)	Not Found	64% (73%)	Not Found	Not Found	Not Found
unknown (AAF33698)	99% (99%)	75% (81%)	82% (88%)	Not Found	34% (50%)	42% (62%)

Figures are reported as percent identity with percent similarity indicated in parenthesis. Blastp was done at the NCBI site except for *M. avium*, which was done at the TIGR site using tblastn. Not found indicates that the gene sequence is not available in public databases.

tis coding sequence, gnd, has similarity to the 6-phophogluconate dehydrogenase genes in E. coli, but the mycobacterial protein is predicted to be about 200 amino acids shorter than the E. coli homolog. The length of non-coding intergenic regions between rpmH – dnaA and dnaA – dnaN is well conserved among the bacteria shown in figure 2. In many bacteria where a functional oriC has been identified, this gene order is conserved and oriC is adjacent to the dnaA gene [9,10,19].

The amino acid sequence of each gene product was compared with the corresponding sequence in *M. paratuberculosis* for all species in this study (Table 2). The data show that while gene order is conserved, the percent identity declines in comparisons with mycobacteria other than *M. avium*. This percent identity declines even further in comparisons with non-mycobacterial sequences such as *S. coelicolor* and *Corynebacteria glutamicum* (Table 2).

Conserved functional motifs in the M. paratuberculosis *putative* oriC

Fuzznuc (EMBOSS; http://www.hgmp.mrc.ac.uk/Software/EMBOSS/index.html) was used to identify potential DnaA boxes in the *M. paratuberculosis oriC* region. The Gram-positive organisms in this study harbor 10 – 30 DnaA boxes (with 1 – 3 mismatches from the consensus sequence TTGTCCACA) flanking the *dnaA* sequence [8,20–23] and 35 were found surrounding the *M. paratuberculosis dnaA* gene (Fig. 3). In addition, a hexameric sequence thought to be recognized by ATP-DnaA (AGATCT) was found in the 3' non-coding sequence adjacent to *dnaA* (Fig. 3b). The significance of additional *dnaA* boxes in *M. paratuberculosis* is likely necessary to open the DNA helix of this GC rich organism (69% GC content).

The *dnaA* gene is divided into four functional domains based on analysis of several *dnaA* mutants [24]. These domains consist of (1) an area near the N-terminus thought be involved in ability of the DnaA protein to aggregate, (2) ATP binding, (3) a domain that maps to a region near the C-terminus and is involved in DNA binding, (4) and a final domain of unknown function, but may bind DnaB. The conserved ATP-binding site that is found in domain III in other bacteria was also located in *M. paratuberculosis* (Fig. 3b). An AT-rich stretch of 19 nucleotides (74% A+T), which in other bacteria serves as the site of local unwinding of DNA after DnaA-DNA interaction, was located in non-coding sequence adjacent to *dnaA* (Fig. 3b). The non-coding sequences flanking *dnaA* are slightly AT-rich in general, relative to the rest of the genome sequence, consistent with findings in other gram-positive bacteria (38% – 40% A/T, vs. ~33% in the entire sequence).

A vast majority of all M. paratuberculosis *K-10 genomic sequence have considerable nucleotide similarity to sequences from the human pathogenic isolate* M. avium *104*

As a basis for all nucleotide comparisons between *M. avium* and *M. paratuberculosis* in this study, an alignment of the 16s rRNA gene was performed. That analysis revealed a 100% nucleotide identity over the entire 1,472-bp gene (data not shown). Likewise, the *oriC* region in *M. paratuberculosis* was found to share a high level of nucleotide identity (~98%) with *M. avium*. Calculation of the rates of total nucleotide diversity (3) and synonymous substitution per synonymous site (ds) and non-synonymous substitution per non-synonymous site (dn) revealed patterns of variation within the range observed from sequence data outside the *oriC* region. These calculations showed a high degree of similarity between the two sequences and a predominance of synonymous over non-synonymous substitutions (Fig. 1). The patterns of nucleotide substitution

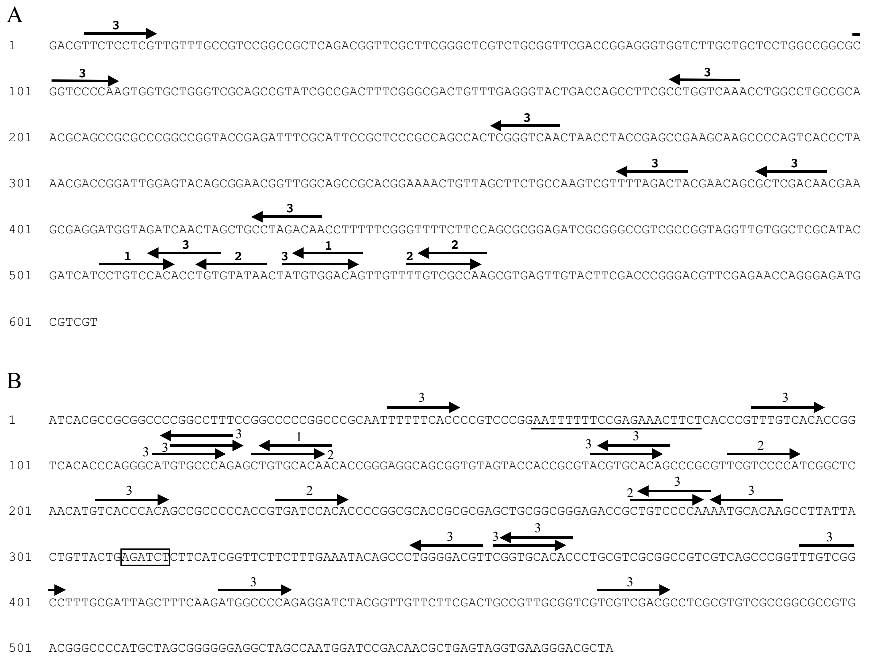
A
1 GACGTTCTCCTCGTTGTTTGCCGTCCGGCCGCTCAGACGGTTCGCTTCGGGCTCGTCTGCGGTTCGACCGGAGGGTGGTCTTGCTGCTCCTGGCCGGCGC
101 GGTCCCCAAGTGGTGCTGGGTCGCAGCCGTATCGCCGACTTTCGGGCGACTGTTTGAGGGTACTGACCAGCCTTCGCCTGGTCAAACCTGGCCTGCCGCA
201 ACGCAGCCGCGCCCGGCCGGTACCGAGATTTCGCATTCCGCTCCCGCCAGCCACTCGGGTCAACTAACCTACCGAGCCGAAGCAAGCCCCAGTCACCCTA
301 AACGACCGGATTGGAGTACAGCGGAACGGTTGGCAGCCGCACGGAAAACTGTTAGCTTCTGCCAAGTCGTTTTAGACTACGAACAGCGCTCGACAACGAA
401 GCGAGGATGGTAGATCAACTAGCTGCCTAGACAACCTTTTTCGGGTTTTCTTCCAGCGCGGAGATCGCGGGCCGTCGCCGGTAGGTTGTGGCTCGCATAC
501 GATCATCCTGTCCACACCTGTGTATAACTATGTGGACAGTTGTTTTGTCGCCAAGCGTGAGTTGTACTTCGACCCGGGACGTTCGAGAACCAGGGAGATG
601 CGTCGT
B
1 ATCACGCCGCGGCCCCGGCCTTTCCGGCCCCCGGCCCGCAATTTTTTCACCCCGTCCCGGAATTTTTTCCGAGAAACTTCTCACCCGTTTGTCACACCGG
101 TCACACCCAGGGCATGTGCCCAGAGCTGTGCACAACACCGGGAGGCAGCGGTGTAGTACCACCGCGTACGTGCACAGCCCGCGTTCGTCCCCATCGGCTC
201 AACATGTCACCCACAGCCGCCCCCACCGTGATCCACACCCCGGCGCACCGCGCGAGCTGCGGCGGGAGACCGCTGTCCCCAAAATGCACAAGCCTTATTA
301 CTGTTACTGAGATCTCTTCATCGGTTCTTCTTTGAAATACAGCCCTGGGGACGTTCGGTGCACACCCTGCGTCGCGGCCGTCGTCAGCCCGGTTTGTCGG
401 CCTTTGCGATTAGCTTTCAAGATGGCCCCAGAGGATCTACGGTTGTTCTTCGACTGCCGTTGCGGTCGTCGTCGACGCCTCGCGTGTCGCCGGCGCCGTG
501 ACGGGCCCCATGCTAGCGGGGGGAGGCTAGCCAATGGATCCGACAACGCTGAGTAGGTGAAGGGACGCTA

Figure 3
Non-coding sequences flanking *M. paratuberculosis dnaA* harbor 35 DnaA boxes. Nucleotide sequence of the *rpmH*-*dnaA* intergenic region (A) and *dnaA*-*dnaN* intergenic region (B) are shown. Sequences matching the DnaA box consensus(TTGTCCACA) with 1 – 3 mismatches are marked with an arrow. In (B), an A/T-rich region is underlined and the potential ATP-DnaA recognition site is boxed.

varied considerably between genes in this region of the genome. For instance, there was complete nucleotide identity in the *rpmH* and *recF* genes and only 94% identity in the gene *rnpA*. To verify that these observed differences were real and not as a result of sequencing errors in the yet unfinished *M. avium* genome, we confirmed the data by resequencing the entire 11 kb region from an isolate clone of *M. avium* and obtained identical results (not shown).

We next determined if the nucleotide identities would remain consistently high when *M. paratuberculosis* sequences outside the *oriC* region were compared with *M. avium*. Sequencing of the *M. paratuberculosis* K-10 cattle isolate is nearing completion in our laboratories and TIGR http://www.tigr.org is in the finishing stages of *M. avium* isolate 104. Beginning with nucleotide number 1 in the *dnaA* coding region of each genome, a comparison of 2 million bases of *M. paratuberculosis* with 2 million bases from *M. avium* by Pustell DNA matrix analysis [25], indicates that genomic similarity continues outside the surrounding *oriC* region (Fig. 4). When evaluating similarities between two sequences of this size, a matrix comparison is the method of first choice. In addition, the matrix method displays matching regions in the context of the sequence as a whole, making it easy to determine if the regions are repeated or inverted. For example, figure 4 shows a large 56.6 kb genomic inversion of the region surrounding nucleotide 350,000. The DNA identity matrix also identified sequences that were present in one genome, but absent in the other as shown by the broken diagonal lines (Fig. 4). These data show remarkable similarity over large regions in both mycobacterial genomes.

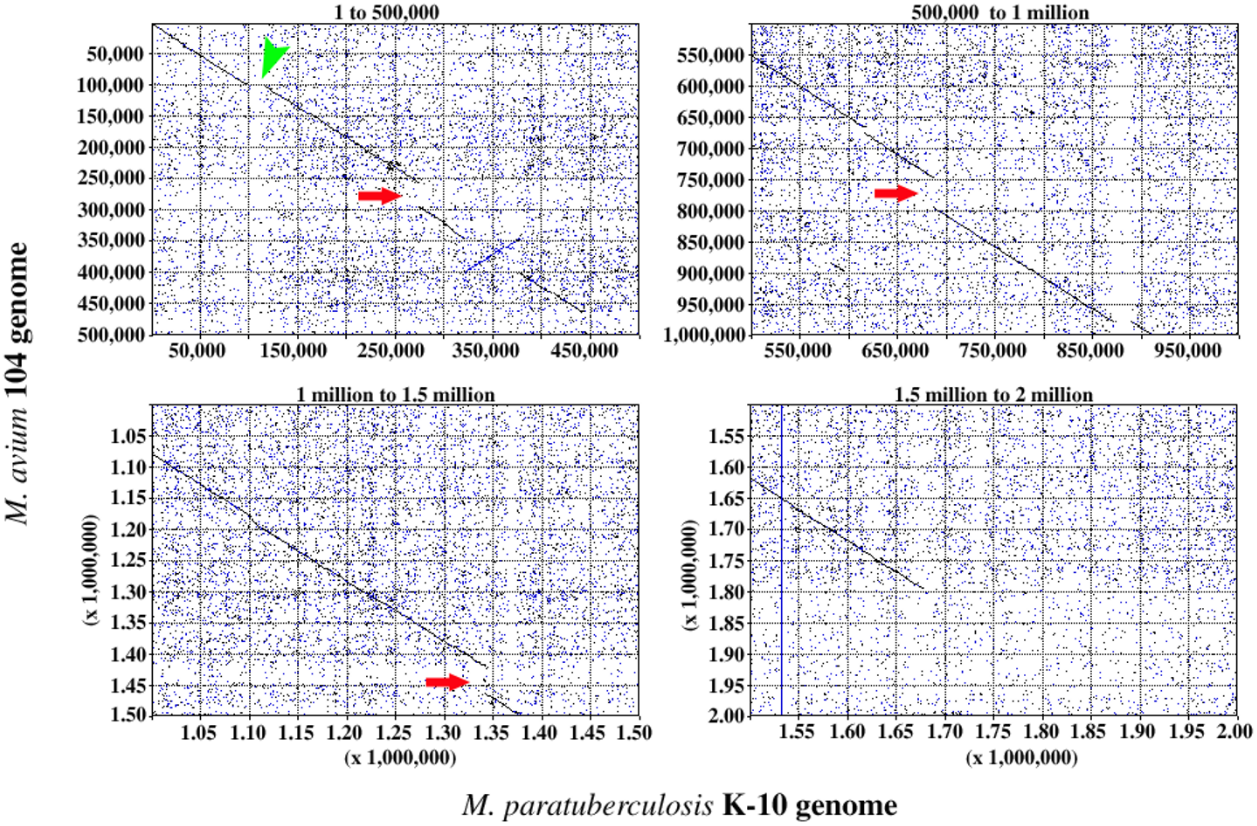

Figure 4

DNA matrix analysis of a contiguous 2 million nucleotide section of the *M. avium* (y-axis) and *M. paratuberculosis* (x-axis) genomes. Four 500,000 nucleotide matrices are shown with the nucleotide segments indicated above each plot. A long unbroken diagonal line from the upper left corner to the lower right corner indicates that the sequences are collinear. The diagonal line (in blue) that runs from the lower left to the upper right at the 350,000 nucleotide region indicates that one sequence is the reverse complement of the other. The arrows (in red) show sequences present in *M. avium* but absent in *M. paratuberculosis* and the arrowhead (in green) shows a sequence represented only in *M. paratuberculosis*. The initial nucleotide in the *dnaA* coding sequence was defined as number one in both genomes for this analysis. The parameters for this DNA identity matrix include: a window size of 30, a minimum percent score of 80, and a hash value of 4.

Finally, we analyzed 548 recombinant clones from a randomly sheared *M. paratuberculosis* small insert library in order to obtain specific rates of nucleotide substitutions. Sequences from these clones represented over 350,000 bp of unique (non-overlapping) *M. paratuberculosis* genomic DNA and comprised 7% of the estimated 5 Mb genome sequence. From this analysis, we estimated the rates of total synonymous and non-synonymous substitutions for 200 fragments that were aligned in-frame and then analyzed with the program NAGV2 [26] using the methods of Nei and Gojobori [27]. The results of these analyses show that the average nucleotide diversity between the two species is 2.59% ± 0.06% (range 0% to 18.8%; median, 1.85% ± 0.05%). The results also show that the average rates of synonymous substitution per synonymous site are 3.38% ± 1.32% (range, 0% to 19.5%; median, 3.5% ± 1.5%). In contrast, the rates of non-synonymous substitution per non-synonymous site were 1.89% ± 0.05% (range, 0% to 12.9%; median 1.3% ± 0.05%). These results not only indicate that the two subspecies have a high degree of nucleotide identity (>97%), but also suggest that the patterns of substitution have favored synonymous substitutions as can be expected from positive selection.

Discussion

With the genome sequencing projects of *M. paratuberculosis* and *M. avium* nearing completion, we have been able to compare large amounts of sequence data for the first time. Our results show substantial nucleotide identity above even that reported previously in the literature [2–4]. Paradoxically, the overall nucleotide identity between these phenotypically distinct mycobacteria appears similar to that observed with two phenotypically identical *Helicobacter pylori* isolates at ≥98% nucleotide identity [28].

The high nucleotide identity shared between *M. paratuberculosis* and *M. avium* directly conflicts with their divergent phenotypic characteristics. Because of strong similarity in the *oriC* region, alternative hypotheses should be tested to explain the growth rate differences between *M. avium* and *M. paratuberculosis*. Genomic rearrangements and the presence of unique genes identified by matrix analysis in this study are two such possibilities that could account for some of the phenotypic differences. We have recently reported on *M. paratuberculosis* coding sequences that are absent in *M. avium* [29]. From an analysis of 48% of the *M. paratuberculosis* genome, only 27 predicted coding sequences were found to be absent in *M. avium*. Therefore, an estimated total of 50–60 *M. paratuberculosis* coding sequences might be absent in *M. avium* following a whole genome analysis. This extremely low number of unique *M. paratuberculosis* genes is in stark contrast to *E. coli* where the MG1655 isolate contains 528 genes not found in the EDL933 isolate [30]. Further analysis of this limited number of unique coding sequences will be critical in developing specific diagnostic reagents. Finally, a detailed analysis of coding sequences unique to each respective mycobacterial genome and their genetic regulatory networks will be necessary to understand the molecular basis for growth rate and other phenotypic differences.

Other potential explanations include the presence of global regulators, insertion sequences, transcription-translation rates, genomic rearrangements and ribosomal RNA operons. Each respective genome possesses insertion elements (IS900, IS1311) at unique loci that could distinctly affect growth difference or other phenotype by insertional mutation. Foley-Thomas et al. [31] compared the expression of the luciferase gene in *M. paratuberculosis* with the fast-growing *M. smegmatis* and concluded that the rates of transcription and translation may not account for the slow growth of *M. paratuberculosis*.

We present evidence for at least one large-scale genomic rearrangement between these two subspecies. This rearrangement consists of a 56.6 kb inversion that contains approximately 61 predicted coding sequences (Bannantine and Kapur, unpublished). Genomic rearrangements such as that described could have a profound effect on phenotype. The presence of multiple copies of ribosomal RNA operons within a genome can be directly attributed to faster growth rate. The increased gene dosage results in more ribosomes and therefore increased protein translational capacity. However, only one rRNA operon is present in each subspecies and this is also true for the fast growers *Mycobacterium abscessus* and *Mycobacterium chelonae* [32]. These fast growing mycobacteria have multiple promoters that increase the transcriptional rate of the rRNA operon to overcome gene dosage limitations [32]. The rRNA operon promoter structures have not been mapped by primer extension for either *M. paratuberculosis* or *M. avium*, but if *M. avium* had multiple functional rRNA operon promoters, that may account for the growth rate differences.

The genetic organization of the origin of replication has been characterized in several Gram-positive pathogens including *B. subtilis*, *S. coelicolor*, *M. tuberculosis*, *M. avium*, *M. leprae*, and *M. smegmatis* [8]. The results of our investigation on the *oriC* region of *M. paratuberculosis* show that each of the 15 primer pairs, designed from *M. avium* sequence data, resulted in the successful amplification and subsequent sequencing of an ~11 kb region of the *M. paratuberculosis* genome. The sequenced region encodes 11 putative proteins, several of which show a high level of identity to proteins that are known or predicted to be involved in DNA replication. However, we found a cluster of substitutions in a region of *rnpA* (data not shown). It is noteworthy that in this region of the gene, each of the nucleotide substitutions results in an amino acid replacement. While mutations in this region of the gene are known to result in dramatic differences in ability of bacteria to respond to environmental stresses [33], the functional significance of these differences between *M. avium* and *M. paratuberculosis* are at present unknown. While these sequencing efforts have revealed a conserved gene order in the *oriC* of Gram-positive bacteria [11], the nucleotide and amino acid identity between *M. paratuberculosis* and *M. avium* in this region is much stronger when compared to other mycobacteria and other Gram-positive bacteria (see Table 2). It is well recognized that the characterization of gene organization in the *oriC* region as well as the complete genome sequence will provide a springboard for addressing questions such as the nature of the slow growth rate of *M. paratuberculosis* as compared to the genetically related rapidly-growing mycobacteria. Progress on these research fronts will improve our chances of understanding and controlling infections caused by *M. paratuberculosis* and related pathogens.

The conservation of functional sequence motifs in the *oriC* of other Gram-positive organisms has provided clues to the mechanism of bacterial replication. For instance, DnaA monomers bind to specific, non-palindromic 9-nucleotide sequences called DnaA boxes, and this interaction is thought to initiate replication. The *oriC* of Gram-positive bacteria typically contains 10 – 30 of these DnaA boxes, often found in non-coding regions flanking the *dnaA* gene. The interaction of DnaA with DnaA boxes promotes the local unwinding of a nearby AT-rich region, providing an entry site for the DnaB/DnaC helicase complex. The *dnaA* gene itself is divided into four domains that differ in the extent of sequence homology [34]. Domain IV is responsible for DnaA box recognition and domain III is a highly conserved region containing the ATP-binding site [13,35]. Domain I participates in cooperative DnaA protein-DNA interactions [36].

The genetic relatedness of *M. paratuberculosis* with other mycobacterial subspecies has been the root cause of the lack of development of *M. paratuberculosis*-specific diagnostic tests. By comparing the genome sequences of both *M. paratuberculosis* and *M. avium*, specific diagnostic tests may be developed and a better understanding of the molecular differences that contribute to unique phenotypes will be obtained. Finally, knowledge of the complete genome sequence of *M. paratuberculosis* is expected to facilitate the identification of diagnostic sequences in this economically significant veterinary pathogen.

Conclusion

With the genomes of *M. paratuberculosis* and *M. avium* nearly completed, investigators will be able to analyze the similarities and differences between these genomes with amazing detail. Through a comparative genomic analysis of over 2 million nucleotides, we have shown that the two subspecies, *avium* and *paratuberculosis*, are highly similar at the gene and nucleotide level. This is in stark contrast to the phenotypic differences that each displays.

Methods

Strains and growth media

A cattle isolate (K-10) of *M. paratuberculosis* [31] has been chosen for genome sequencing studies. The organism was grown in Middlebrook 7H9 broth supplemented with OADC (Difco Laboratories, Detroit, MI), Tween 80, and mycobactin J (Allied Monitor, Fayette, MO) as described by Bannantine et al. [37]. *M. avium* strain 104 was grown in Middlebrook 7H9 broth. DNA was extracted using the Qiagen QIAamp Tissue Kit (Chatsworth, CA).

Primer design and amplifications

A web-interfaced program, Primer3 http://www-genome.wi.mit.edu/cgi-bin/primer/primer3_www.cgi, was used. Primers were designed based on available *M. avium* strain 104 genomic sequence data http://www.tigr.org for the amplification of 11 genes in a contiguous ~11 kb *M. paratuberculosis* fragment surrounding the putative origin of replication (*oriC*). By this strategy, a total of 15 primer pairs were constructed for the amplification of 15 minimally overlapping fragments of ~800 bp in length for this region of the *M. paratuberculosis* genome. Amplification reactions included the high fidelity DNA polymerase, Pfu (Stratagene, La Jolla, CA) and an annealing temperature of 58°C.

Library construction

A random 2.2-kb insert library of *M. paratuberculosis* K-10 has been constructed as follows. Total *M. paratuberculosis* genomic DNA was isolated and randomly sheared using a nebulizer and compressed nitrogen according to protocols developed by Bruce Roe's laboratory http://www.genome.ou.edu. The resulting DNA fragments were separated by gel electrophoresis and fragments in the range of 2.1–2.2 kb were purified. After polishing the ends of the fragments using Klenow (New England Biolabs, Beverly, MA), they were cloned into *SmaI*-restricted/CIAP pUC18 vector. The resulting library was >90% recombinant and contained more than 50,000 independent recombinant clones.

DNA Sequencing and Analysis

The DMSO protocol (ABI Automated DNA Sequencing Chemistry Guide, ABI, Foster City, CA) was implemented for carrying out the sequencing reactions and data were collected using ABI 377 automated DNA sequencers at the Advanced Genetic Analysis Center at the University of Minnesota. The data was analyzed using the DNAStar (Madison, WI) package and Artemis [15]. Rates of synonymous and non-synonymous substitution were calculated by the un-weighted method of Nei and Gojobori [27]. Pustell DNA matrix analysis [25] was performed using MacVector version 7.1 software.

Nucleotide Sequence Accession Number

The GenBank accession number for the *M. paratuberculosis* 11-kb *oriC* region is AF222789. The *M. paratuberculosis* random sequences can be accessed via the *M. paratuberculosis* genome project website: http://www.cbc.umn.edu/ResearchProjects/AGAC/Mptb/Mptbhome.html.

Acknowledgements

This work was funded by Agricultural Research Service intramural funds and USDA-NRI grants to V.K. and J.P.B. We thank Robert Fleischmann and coworkers at TIGR for their efforts in sequencing the *M. avium* genome.

References

1. Thorel MF, Krichevsky M and Levy-Frebault VV **Numerical taxonomy of mycobactin-dependent mycobacteria, emended description of *Mycobacterium avium*, and description of *Mycobacterium avium* subsp. *avium* subsp. nov., Mycobacterium avium** *Int J Syst Bacteriol* 1990, **40:**254-260
2. Hurley SS, Splitter GA and Welch RA **Development of a diagnostic test for Johne's disease using a DNA hybridization probe** *J Clin Microbiol* 1989, **27:**1582-1587
3. Saxegaard F, Baess I and Jantzen E **Characterization of clinical isolates of *Mycobacterium paratuberculosis* by DNA-DNA hybridization and cellular fatty acid analysis** *Apmis* 1988, **96:**497-502

4. Yoshimura HH and Graham DY **Nucleic acid hybridization studies of mycobactin-dependent mycobacteria** *J Clin Microbiol* 1988, **26:**1309-1312
5. Harris NB and Barletta RG ***Mycobacterium avium* subsp. *paratuberculosis* in Veterinary Medicine** *Clin Microbiol Rev* 2001, **14:**489-512
6. Horsburgh CR Jr ***Mycobacterium avium* complex infection in the acquired immunodeficiency syndrome** *N Engl J Med* 1991, **324:**1332-1338
7. Qin MH, Madiraju MV, Zachariah S and Rajagopalan M **Characterization of the oriC region of *Mycobacterium smegmatis*** *J Bacteriol* 1997, **179:**6311-6317
8. Salazar L, Fsihi H, de Rossi E, Riccardi G, Rios C, Cole ST and Takiff HE **Organization of the origins of replication of the chromosomes of *Mycobacterium smegmatis, Mycobacterium leprae* and *Mycobacterium tuberculosis* and isolation of a functional origin from *M. smegmatis*** *Mol Microbiol* 1996, **20:**283-293
9. Skarstad K and Boye E **The initiator protein DnaA: evolution, properties and function** *Biochim Biophys Acta* 1994, **1217:**111-130
10. Smith DW, Yee TW, Baird C and Krishnapillai V **Pseudomonad replication origins: a paradigm for bacterial origins?** *Mol Microbiol* 1991, **5:**2581-2587
11. Ogasawara N and Yoshikawa H **Genes and their organization in the replication origin region of the bacterial chromosome** *Mol Microbiol* 1992, **6:**629-634
12. Yoshikawa H and Ogasawara N **Structure and function of DnaA and the DnaA-box in eubacteria: evolutionary relationships of bacterial replication origins** *Mol Microbiol* 1991, **5:**2589-2597
13. Koonin EV **A common set of conserved motifs in a vast variety of putative nucleic acid-dependent ATPases including MCM proteins involved in the initiation of eukaryotic DNA replication** *Nucleic Acids Res* 1993, **21:**2541-2547
14. Lobry JR **Asymmetric substitution patterns in the two DNA strands of bacteria** *Mol Biol Evol* 1996, **13:**660-665
15. Rutherford K, Parkhill J, Crook J, Horsnell T, Rice P, Rajandream MA and Barrell B **Artemis: sequence visualization and annotation** *Bioinformatics* 2000, **16:**944-945
16. Brown JW and Pace NR **Ribonuclease P RNA and protein subunits from bacteria** *Nucleic Acids Res* 1992, **20:**1451-1456
17. Courcelle J, Carswell-Crumpton C and Hanawalt PC **recF and recR are required for the resumption of replication at DNA replication forks in *Escherichia coli*** *Proc Natl Acad Sci U S A* 1997, **94:**3714-3719
18. Reece RJ and Maxwell A **DNA gyrase: structure and function** *Crit Rev Biochem Mol Biol* 1991, **26:**335-375
19. Fujita MQ, Yoshikawa H and Ogasawara N **Structure of the dnaA region of *Pseudomonas putida*: conservation among three bacteria, Bacillus subtilis, *Escherichia coli* and *P. putida*** *Mol Gen Genet* 1989, **215:**381-387
20. Calcutt MJ and Schmidt FJ **Conserved gene arrangement in the origin region of the *Streptomyces coelicolor* chromosome** *J Bacteriol* 1992, **174:**3220-3226
21. Madiraju MV, Qin MH, Yamamoto K, Atkinson MA and Rajagopalan M **The dnaA gene region of *Mycobacterium avium* and the autonomous replication activities of its 5' and 3' flanking regions** *Microbiology* 1999, **145(Pt 10):**2913-2921
22. Ogasawara N, Moriya S and Yoshikawa H **Initiation of chromosome replication: structure and function of oriC and DnaA protein in eubacteria** *Res Microbiol* 1991, **142:**851-859
23. Rajagopalan M, Qin MH, Nash DR and Madiraju MV ***Mycobacterium smegmatis* dnaA region and autonomous replication activity** *J Bacteriol* 1995, **177:**6527-6535
24. Sutton MD and Kaguni JM **The *Escherichia coli dnaA* gene: four functional domains** *J Mol Biol* 1997, **274:**546-561
25. Pustell J and Kafatos FC **A convenient and adaptable package of computer programs for DNA and protein sequence management, analysis and homology determination** *Nucleic Acids Res* 1984, **12:**643-655
26. Kapur V, Kanjilal S, Hamrick MR, Li LL, Whittam TS, Sawyer SA and Musser JM **Molecular population genetic analysis of the streptokinase gene of *Streptococcus pyogenes*: mosaic alleles generated by recombination** *Mol Microbiol* 1995, **16:**509-519
27. Nei M and Gojobori T **Simple methods for estimating the numbers of synonymous and nonsynonymous nucleotide substitutions** *Mol Biol Evol* 1986, **3:**418-426
28. Alm RA, Ling LS, Moir DT, King BL, Brown ED, Doig PC, Smith DR, Noonan B, Guild BC, deJonge BL, Carmel G, Tummino PJ, Caruso A, Uria-Nickelsen M, Mills DM, Ives C, Gibson R, Merberg D, Mills SD, Jiang Q, Taylor DE, Vovis GF and Trust TJ **Genomic-sequence comparison of two unrelated isolates of the human gastric pathogen *Helicobacter pylori*** *Nature* 1999, **397:**176-180
29. Bannantine JP, Baechler E, Zhang Q, Li L and Kapur V **Genome Scale Comparison of *Mycobacterium avium* subsp. *paratuberculosis* with *Mycobacterium avium* subsp. *avium* Reveals Potential Diagnostic Sequences** *J Clin Microbiol* 2002, **40:**1303-1310
30. Perna NT, Plunkett G 3rd, Burland V, Mau B, Glasner JD, Rose DJ, Mayhew GF, Evans PS, Gregor J, Kirkpatrick HA, Posfai G, Hackett J, Klink S, Boutin A, Shao Y, Miller L, Grotbeck EJ, Davis NW, Lim A, Dimalanta ET, Potamousis KD, Apodaca J, Anantharaman TS, Lin J, Yen G, Schwartz DC, Welch RA and Blattner FR **Genome sequence of enterohaemorrhagic *Escherichia coli* O157:H7** *Nature* 2001, **409:**529-533
31. Foley-Thomas EM, Whipple DL, Bermudez LE and Barletta RG **Phage infection, transfection and transformation of *Mycobacterium avium* complex and *Mycobacterium paratuberculosis*** *Microbiology* 1995, **141:**1173-1181
32. Gonzalez-y-Merchand JA, Garcia MJ, Gonzalez-Rico S, Colston MJ and Cox RA **Strategies used by pathogenic and nonpathogenic mycobacteria to synthesize rRNA** *J Bacteriol* 1997, **179:**6949-6958
33. Kirsebom LA, Baer MF and Altman S **Differential effects of mutations in the protein and RNA moieties of RNase P on the efficiency of suppression by various tRNA suppressors** *J Mol Biol* 1988, **204:**879-888
34. Fujita MQ, Yoshikawa H and Ogasawara N **Structure of the dnaA and DnaA-box region in the *Mycoplasma capricolum* chromosome: conservation and variations in the course of evolution** *Gene* 1992, **110:**17-23
35. Roth A and Messer W **The DNA binding domain of the initiator protein DnaA** *Embo J* 1995, **14:**2106-2111
36. Messer W, Blaesing F, Jakimowicz D, Krause M, Majka J, Nardmann J, Schaper S, Seitz H, Speck C, Weigel C, Wegrzyn G, Welzeck M and Zakrzewska-Czerwinska J **Bacterial replication initiator DnaA. Rules for DnaA binding and roles of DnaA in origin unwinding and helicase loading** *Biochimie* 2001, **83:**5-12
37. Bannantine JP and Stabel JR **HspX is present within *Mycobacterium paratuberculosis*-infected macrophages and is recognized by sera from some infected cattle** *Vet Microbiol* 2000, **76:**343-358